

RESEARCH

Open Access



# Sedimentological and petrographic analysis of Neogene quaternary continental deposits in Argoub Kemellal Oum El Bouaghi northeastern Algeria evidence for a fluvial to lacustrine transition

Meguellati Asma<sup>1</sup>, Djerrab Abderrezak<sup>2</sup>, Khiari Abdelkader<sup>1</sup>, Gallet Xavier<sup>3</sup>, Dinar Haythem<sup>4</sup>, Garah Abdelmoumen<sup>5</sup>, Riheb Hadji<sup>6</sup>, Imtiyaz Akbar Najar<sup>7\*</sup>, Raudhah Ahmadi<sup>7\*</sup> and Nadeem A. Khan<sup>8</sup>

\*Correspondence:  
Imtiyaz Akbar Najar  
imtiyaznajar999@gmail.com  
Raudhah Ahmadi  
araudhah@unimas.my

Full list of author information is available at the end of the article

## Abstract

The Argoub Kemellal dome, located south of Oum El Bouaghi in northeastern Algeria, preserves a rich sedimentary archive documenting the paleoenvironmental evolution of the Neogene-Quaternary period. This study aims to reconstruct the paleogeographic development of the region by examining the interplay between sedimentary processes and environmental changes, particularly the transition from fluvial to lacustrine conditions. A multidisciplinary approach combining petrographic and sedimentological analyses was applied. Techniques included granulometric and calcimetric measurements, thin-section petrography, and both morphoscopic and scanning electron microscope (SEM) studies of quartz grains. The geological sequence comprises Miocene-aged detrital deposits overlain by Pliocene to Quaternary carbonate formations. Sedimentary formations document a transition from high-energy fluvial conditions to calmer lacustrine environments, driven by climatic change. Notably, calcium carbonate (CaCO<sub>3</sub>) content increases upward from 13% at the base to 57% at the top, highlighting the shift toward carbonate-dominated lacustrine sedimentation. These results illustrate how climate forcing shaped sedimentary environments over time and contribute to reconstructing the Neogene-Quaternary paleogeography of the studied region. The finding underscores the value of continental deposits as sensitive geological archives of past environmental and climatic conditions.

## Article highlights

- i. The study shows environmental changes and a transition from river to lake environments.
- ii. Carbonate content increased upward, revealing the development of lacustrine sedimentation.
- iii. The sequence helps reconstruct the Neogene-Quaternary paleogeography of the region.



**Keywords** Continental carbonate, Argoub Kemellal, Grain size analysis, Paleoenvironment, Lacustrine

## 1 Introduction

Neogene-Quaternary continental deposits represent essential archives for reconstructing terrestrial paleoenvironments and landscape evolution [1]. In North Africa, these deposits record the interaction between tectonic activity and sedimentary processes during a period marked by major global and regional environmental changes [2]. Among these deposits, fluvio-lacustrine detrital sediments and continental carbonates are particularly informative, as fluvial systems preserve signals of sediment supply, transport energy, and hydrological variability [3–5], while continental carbonates form under specific hydrological and climatic conditions and provide sensitive records of chemical and biological processes in lacustrine environments [6]. Together, these sedimentary systems allow reconstruction of past depositional environments and their responses to external forcings.

At the regional scale, sedimentation during the Neogene-Quaternary in northeastern Algeria was mainly controlled by (1) tectonic activity related to Atlas uplift and regional fault systems, (2) climatic fluctuations between humid and arid phases, and (3) hydrological changes influencing drainage networks and the evolution of lacustrine basins. Major events such as the Messinian Salinity Crisis profoundly modified Mediterranean connectivity and regional drainage patterns during the Miocene [7–12], whereas humid phases during the Pliocene, associated with intensified African monsoon activity, promoted lacustrine expansion and reduced clastic input [13, 14]. Understanding how these events affected depositional processes and biodiversity within individual basins remains essential for refining regional paleogeographic models [15, 16].

Although previous research conducted in the Oum El Bouaghi region has successfully documented its morpho-structural framework and tectonic evolution [17–22], as well as hydrogeological and geomorphological aspects [18, 23, 24], no detailed sedimentological or petrographic study of the Neogene-Quaternary unconsolidated deposits has yet been carried out. Consequently, sedimentary facies, textural characteristics, grain-size distributions, and carbonate contents remain poorly documented, limiting our understanding of the respective roles of tectonic and climatic controls on sedimentation during this key stratigraphic interval.

By contrast, systematic sedimentological investigations in neighboring regions, particularly in Tunisia and Morocco, have significantly improved reconstructions of fluvio-lacustrine environments and sedimentary dynamics [25–27]. Elsewhere in North Africa, Miocene successions have been constrained using integrated biostratigraphic, magnetostratigraphic, radiometric, and lithostratigraphic approaches [28, 29]. In Algeria, several studies have addressed fluvio-lacustrine deposits [30], radioisotopic dating of Quaternary gastropods [31–33] archaeological environments [33, 34], fluvial terraces [35, 36], marine terraces [33, 37, 38], and Miocene sedimentary sequences through micropaleontological analyses [39]. Despite these contributions, no comprehensive sedimentological and petrographic investigation has yet focused on the Oum El Bouaghi sector.

This study addresses this gap by presenting an integrated sedimentological and petrographic analysis of the Neogene-Quaternary deposits of the Argoub Kemellal dome,

located south of Oum El Bouaghi within the para-autochthonous North Aurès domain. Using a multidisciplinary approach combining granulometric analyses, calcimetry, thin-section petrography, and morphoscopic and exoscopic analyses of quartz grains, this work aims to characterize sedimentary facies, reconstruct depositional environments, and evaluate the relative influence of climatic and tectonic drivers. The results provide new constraints on the Neogene-Quaternary paleogeographic evolution of northeastern Algeria and contribute to regional correlations across North Africa.

### 1.1 The regional setting

The Oum El Bouaghi region in northeastern Algeria is distinguished by its diverse and striking physical features (Fig. 1). The landscape is predominantly composed of extensive plains at elevations ranging from 800 to 950 m.

A notable geological feature is the Argoub Kemellal outcrop, which stands prominently among adjacent mountain ranges, including Jebel Sidi R'ghis to the north, Jebel Guellif to the southwest, and Jebel Tarf to the south. The depressions between these mountains are home to salt lakes, such as Garaet Guellif and Garaet Tarf (Fig. 2).

Hydrographically, the region exhibits an endorheic network, with water flow directed toward the chotts located in the southeast and south. North of the Sidi R'ghis–Touzelline axis, wadis flow northward. The southeastern slope is divided into four hydraulic basins. The first basin, drained by Oued Meroui, is situated east of the town and encompasses approximately 650 hectares. The second basin, drained by Oued Kouider, is located to the northwest and covers 406 hectares. The third basin lies south of the second, while the fourth basin, covering around 350 hectares, drains into agricultural land.

Geologically, Oum El Bouaghi belongs to the para-autochthonous North Auresian domain, positioned along the northern margin of the Atlasic system [18, 28]. The region has been significantly influenced by Alpine tectonics, particularly a compressional regime oriented from north to south and northwest to southeast, which has persisted

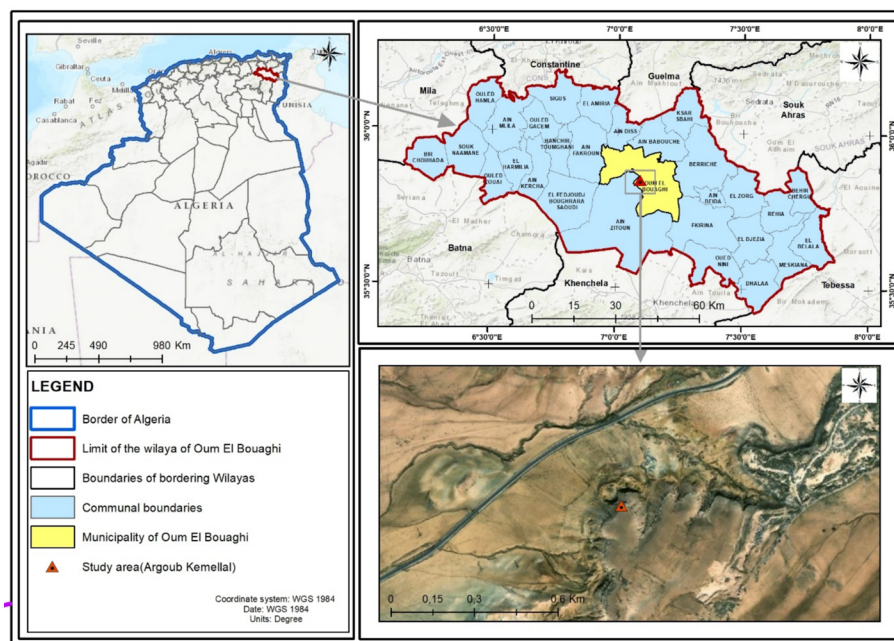


**Fig. 1** The geographical location of the study area of Argoub Kemellal (Oum El Bouaghi, Algeria)

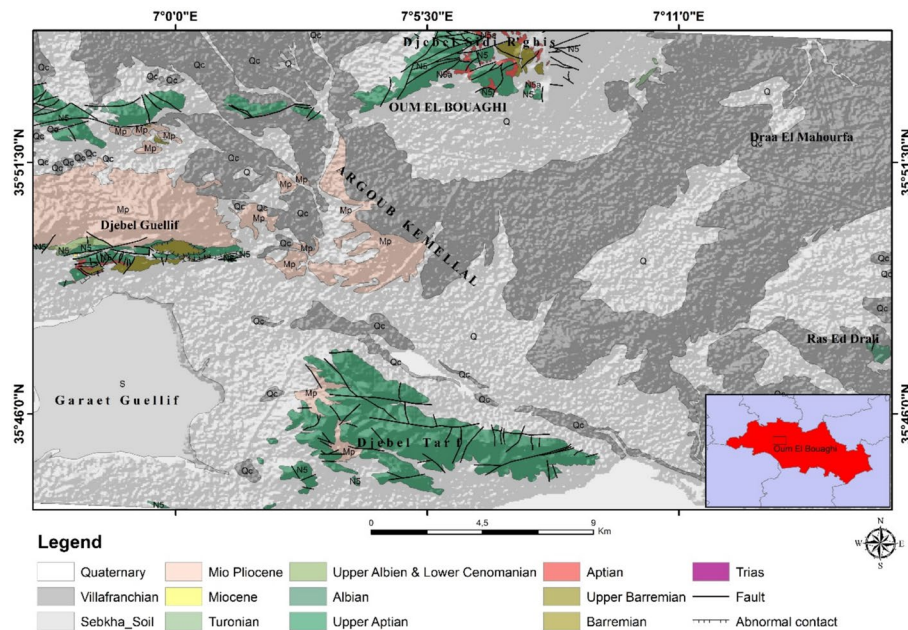


**Fig. 2** geological map of study area (source [18])

from the early Cenozoic to the Quaternary period [19, 33]. This tectonic activity has contributed to the formation of characteristic mountainous landforms, including Jebel Sidi R'ghis, Jebel Guellif, and Jebel Tarf, as well as extensive steppe plains interspersed with salt lakes (Sebkhha environments).

## 1.2 Lithostratigraphy

The lithostratigraphic framework of the Oum El Bouaghi region encompasses a stratigraphic succession extending from the Triassic to the Quaternary, documenting a range of depositional settings and tectono-sedimentary processes. Of particular interest to this study are the Mio–Pliocene and Quaternary deposits. Triassic strata are characterized by pink, brecciated gypsum, indicative of evaporitic depositional conditions. The Cretaceous succession exhibits marked lithological heterogeneity: Barremian units consist of fine-grained sandstones intercalated with calcareous–dolomitic layers; Aptian deposits are dominated by massive limestones and dolomites; Albian sequences comprise grey marls with interbedded sandstones; and Turonian strata are typified by light-colored biomicrites, reflecting shallow marine carbonate sedimentation.

During the Mio-Pliocene, outcrops at Jebel Guellif are characterized by red polygenic conglomerates interspersed with clayey layers, overlain by grey marls, additional conglomerates, and lacustrine limestones that can reach several hundred meters in thickness [18]. The Upper Turolian (Messinian) is marked by deposits of clay, sandstone, brown clay, and marl, which represent the only known Upper Turolian deposits in North Africa [19]. The Quaternary period is distinguished by a variety of formations, including scree deposits, recent alluvium in wadi valleys, extensive polygenic glacia, thick Villafranchian limestone crusts, periodically flooded salt sebkhas, and dune systems situated east of Garaet Guellif (Fig. 2).

The analyzed section is taken from the Argoub Kemellal dome (Fig. 1), located approximately 1 km south of Oum El Bouaghi, along the Ain Zitoune road. The geographical

coordinates are approximately 35°50' north latitude and 7°36' east longitude. The Argoub Kemellal dome corresponds to an anticlinal structure extending eastward, characterized by limestone layers inclined at angles between 05° and 10° toward the east, which cap its summit. This structural formation is the result of a predominantly north–south compressional regime occurring at the end of the Late Neogene, leading to the development of dextral reverse strike-slip faults with an east–west orientation.

Within Argoub Kemellal, two primary lithological units have been identified, as described by [18–20]. The first unit is a detrital fluvial deposit from the Upper Miocene period, measuring several tens of meters in thickness. It consists of grey clays and marls that transition to sandy layers toward the top, followed by slightly silty, yellowish sands exhibiting cross-bedding structures indicative of ancient channel fills. The rapid variation in Late Neogene thickness is considered non-tectonic. A brown clay layer caps this sequence, the Pliocene succession includes sandstones, sands, and conglomerates, overlain by purple-brown pelites and beige to grey marls, concluding with detrital beds containing small encrusted pebbles and sand [19]. The Pliocene succession described westward is located approximately 1 km west of the measured section.

The second unit is a carbonate formation dating from the upper Neogene to the Quaternary, ten meters thick, indicative of a palustrine or lacustrine depositional environment. It comprises light to slightly pinkish limestones in metric beds, underlain by gypsiferous marls. This carbonate unit contains cavities, calcite-filled desiccation cracks, and detrital quartz grains. Climatic conditions are believed to have significantly influenced the sedimentation of this sequence, with the lower portion forming under warm, arid conditions, while the upper levels suggest deposition during a warmer and more humid phase [18, 19].

The sedimentary succession of Argoub Kemellal provides an essential reference for understanding Neogene-Quaternary paleoenvironments in the Maghreb. Our findings corroborate regional models of continental sedimentation and paleoclimate evolution as established by [25, 26] and [27] with shared features such as palustrine carbonates, conglomeratic lags, and evidence for episodic emersion and diagenesis. However, the Argoub Kemellal record uniquely details the stratigraphic transition from fluvial to lacustrine conditions during the Late Neogene-Quaternary, a phase that appears slightly younger than similar transitions in Tunisia and Morocco. This diachronous pattern reflects localized responses to climate forcing and tectonic activity, underscoring the complexity of paleogeographic evolution across North Africa during this period. By integrating macro- and microfacies data, this study refines the timeline and environmental context of Neogene-Quaternary paleoclimatic change in the region.

## **2 Material and methods (methodology)**

### **2.1 Integrating petrographic and sedimentological analyses**

The methodology adopted in this study is based on an integrated approach combining petrographic and sedimentological analyses to characterize the continental deposits of the investigated area. Field campaigns were first conducted to examine the geological features, with particular attention given to vertical facies variations. These observations enabled the establishment of a representative stratigraphic section and the subdivision of the deposits into nine distinct stratigraphic levels. Sampling was carried out starting from Level 03, as the first two levels did not exhibit significant sedimentary features

associated with the fluvial or lacustrine environments under study. A total of 33 samples were collected. The selected levels were those that best preserved primary sedimentary structures and were representative of the depositional settings. To minimize the effects of diagenesis, samples were collected from fresh outcrops or by digging slightly into the deposits to access minimally altered material.

Petrographic analysis was conducted on seven samples, corresponding to sandstones (02 and 17) and limestones (30, 31, 32, 33, 34). Thin sections were prepared by cutting samples with a diamond saw, mounting them on glass slides, and grinding them to a standard thickness of 30  $\mu\text{m}$ . Observations under a polarizing microscope focused on describing sedimentary structures, identifying mineralogical composition, and documenting key diagenetic features [40, 41].

Granulometric analyses were performed on the <2 mm fraction using a Mastersizer 2000 laser diffraction particle size analyzer at the **Muséum national d' Histoire naturelle (Paris)**. Each sample was analyzed both in its raw state and after carbonate removal using a dilute acetic acid solution (05%), which allowed the dissolution of carbonate components without altering the morphology of detrital grains. Conventional statistical parameters (mean grain size, sorting, skewness, kurtosis) were calculated from percentile values following [42–47], to characterize grain-size distributions and infer depositional energy and sediment transport dynamics [44]. Only the essential definitions of these indices were retained to interpret the overall granulometric trends: mean grain size reflecting transport energy, sorting indicating hydrodynamic stability, and skewness and kurtosis providing insights into sediment supply characteristics.

Carbonate content was determined at LNHC Laboratoire national de l'habitat et de la construction (Oum El Bouaghi) using a Bernard calcimeter. The method is based on measuring the volume of  $\text{CO}_2$  released when the sample reacts with hydrochloric acid, compared with a reference volume produced by pure calcite.

Morphoscopic analysis of quartz grains, cold-decarbonated and sieved in the 0.25–0.5 mm fraction, was performed under a binocular microscope ( $\times 50$ ). Grain shape, surface luster, and edge preservation were described to infer transport distance and depositional energy.

Finally, exoscopic observations using scanning electron microscopy (SEM) were conducted at **CRAPC Centre de Recherche Scientifique et Technique en Analyses Physico-Chimiques (Batna)**. Cleaned and gold- or carbon-coated grains were examined with an accelerating voltage of 10–20 kV to identify surface microtextures such as percussion marks, dissolution pits, and siliceous coatings. These features contributed to refining interpretations of sediment transport mechanisms and depositional processes [44, 48, 49].

### 3 Results

#### 3.1 Lithostratigraphy of the Argoub Kemellal section

The lithostratigraphic succession of the Argoub Kemellal section was detailed in order from the bottom up, showing how the deposits changed from detrital to carbonated throughout time (Fig. 3 and 6).

**Basal Unit:** This is composed of soft, plastic marls that are highly weathered and display a light gray to whitish coloration. The marls are approximately 10 m thick and mark the onset of sedimentation.

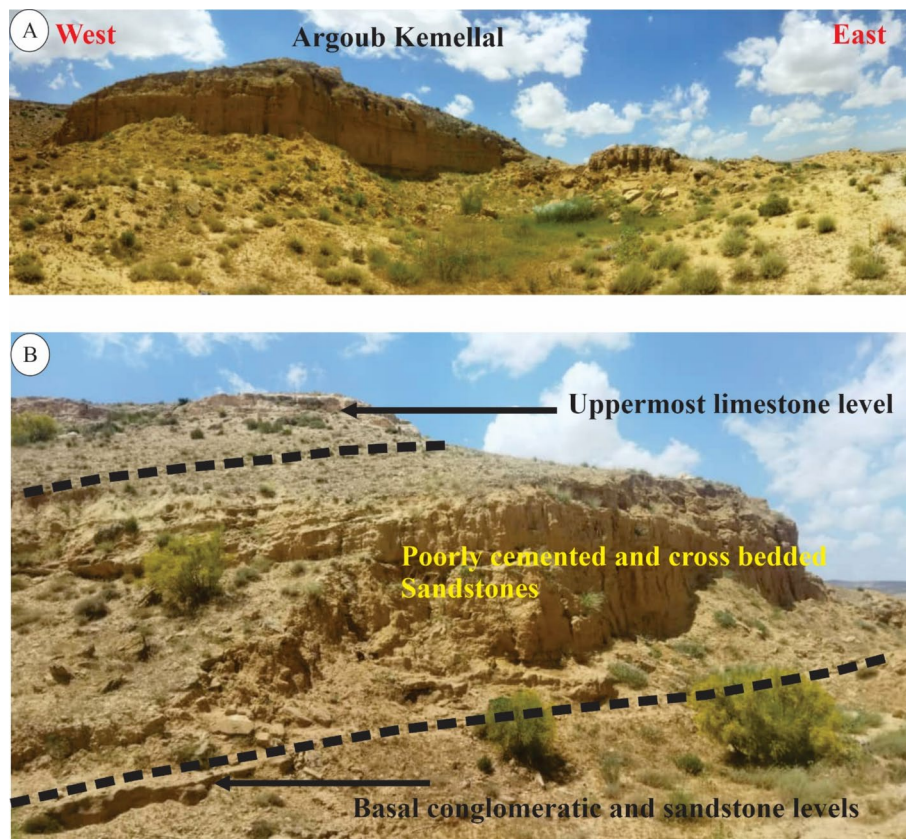


**Fig. 3** **A:** Panoramic view of the study area (Argoub Kemellal), **B:** Panoramic view showing basal conglomerate and sandstone levels, poorly cemented sandstones with cross-bedding, and upper limestone layers

**Basal conglomerate Bed:** A polygenic conglomerate; containing quartz grains and pebbles and carbonate clasts sourced from pre-existing rocks, contain well-rounded clasts ranging in size from a few millimeters to several centimeters (Fig. 3B). These clasts are embedded in a sandy matrix of low hardness. The bed is thin ( $\leq 10$  cm) and exhibits voids likely due to post-depositional erosion. Its color varies from grayish to yellowish tones.

**Coarse Sandstone Layer:** This unit contains large quartz grains (mostly millimetric, occasionally centimetric) with a yellow to grey-brown hue. It is characterized by well-developed stratification, starting with horizontal lamination and transitioning to cross-lamination, forming distinct cross-stratification. Thickness:  $\sim 50$  cm.

**Compacted Sand Layer:** Composed of beige, well-compacted sandstone forming a dense and coherent unit, approximately 5 m thick.

**Sandy Marl:** A homogeneous deposit of fine-grained sandy marl with a crumbly texture and consistent beige coloration. Thickness: 80 cm.

**Marly Unit with Carbonate Beds:** Composed of brownish marls interbedded with centimeter-thick carbonate layers lacking visible stratification (Fig. 4). This unit reaches 4.5 m in thickness.

**Fine-Grained Sandstone:** Finer than the sandstone in level 3, this unit ranges in color from whitish to greyish hue and exhibits both horizontal as well as cross-laminated structures, its thickness is approximately 1m.

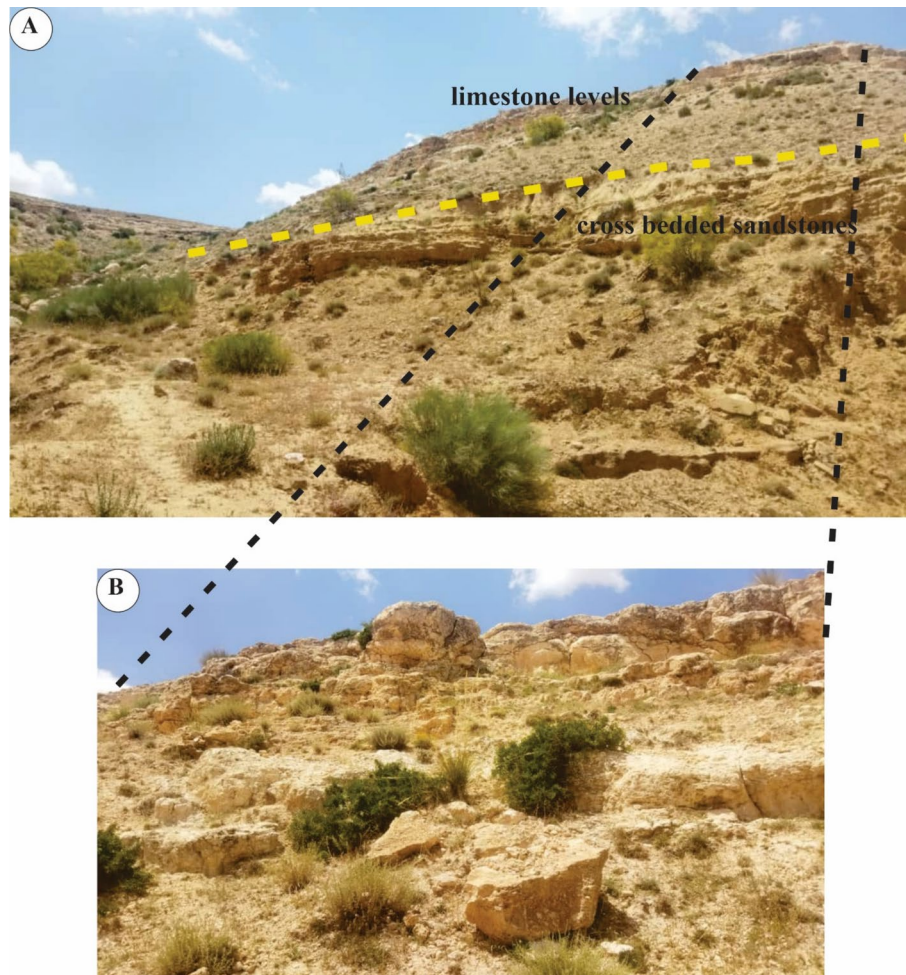


**Fig. 4** A: Panoramic view of cross-bedded sandstones and limestone layers, B: Intensely fractured limestone

Upper Carbonate-Marl Alternation: Begins with a weathered, fractured bed of whitish limestone followed by an alternation of friable, light beige marls and marly-limestone beds in light grey. The marls vary in thickness (several tens of cm), while marl-limestone layers may exceed 1 m. Toward the top, the sequence becomes predominantly calcareous, capped by a 6.6 m thick massive whitish limestone bed (Fig. 5, 6).

### 3.1.1 Microscopic description

Microscopic examination of thin sections from limestones and sandstones reveals a range of continental carbonate facies, with distinct textural and compositional features indicative of subaqueous conditions and episodic emersion.

**3.1.1.1 Sandstones** The sandstones are poorly to moderately cemented, facilitating the observation of their detrital framework. Grains are dominantly angular to sub-angular quartz, ranging from 0.5 mm to over 2 mm. Most grains are monocrystalline, though a minority is polycrystalline (Fig. 7E, F). The cement is composed mainly of ferruginous and clay minerals, distributed discontinuously. Ferruginous cement often appears in red-stained intergranular areas (Fig. 7E), and spherical iron-rich structures, resembling eryth-

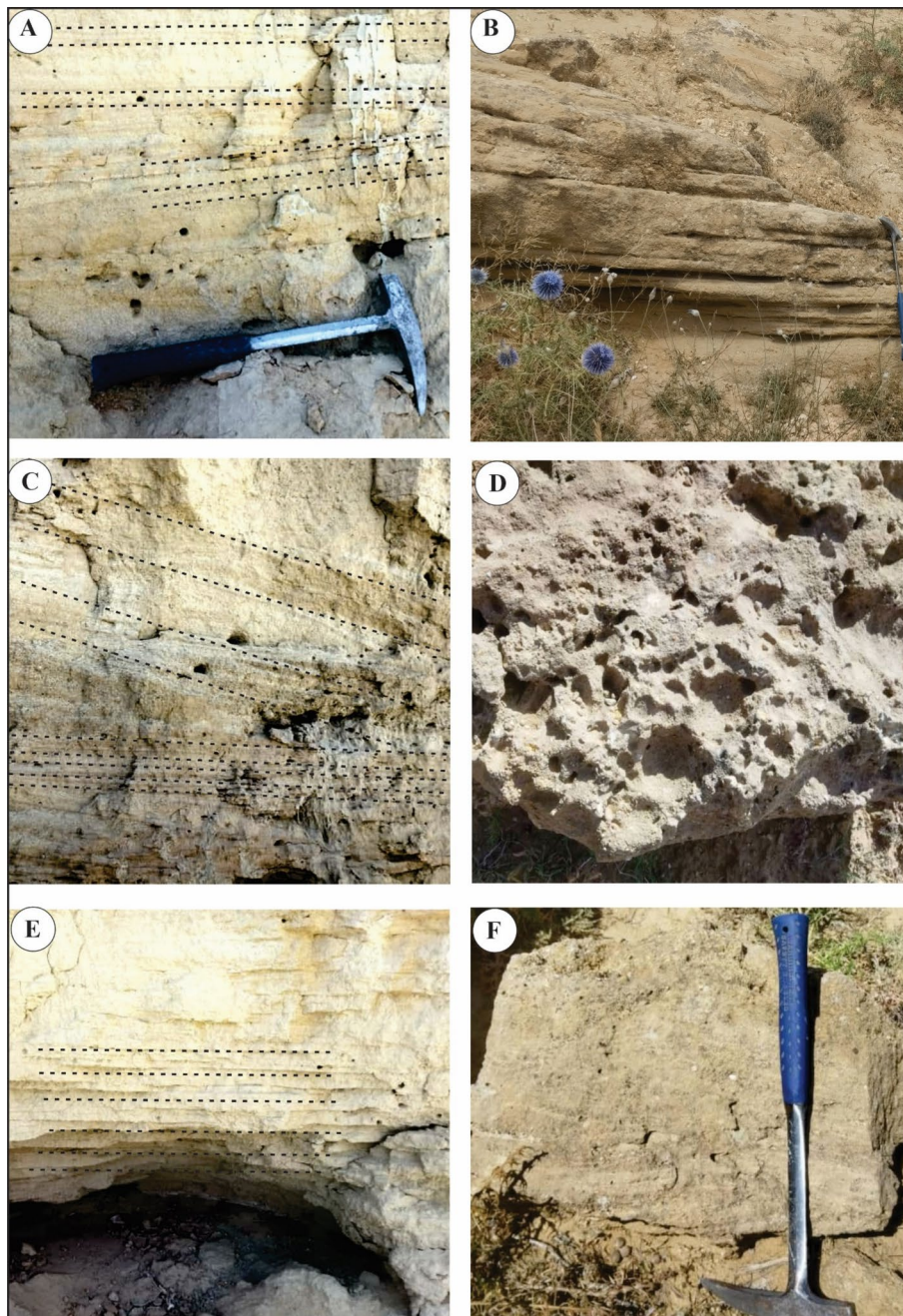


**Fig. 5** **A:** Poorly cemented sandstones with Cross bedding, **B:** Field view of horizontal bedding in basal sandstone (scale: geologist's hammer), **C:** Cross-bedding in sandstones, **D:** Conglomerate level of Argoub Kemellal. **E:** Horizontal-planar laminations in sandstones, **F:** Sandstone with quartz grains

rocytes, are common (Fig. 7F). Clay content comprises about 30–35% of the thin section area and can occur as dispersed argillaceous cement (Fig. 7E, black line).

**3.1.1.2 Limestones** Thin sections of limestones reveal the presence of intramicritic fenestrae, with vugs and keystone structures infilled by micrite containing intraclasts and angular quartz grains (Fig. 7A). Desiccation features such as sheet cracks and intense recrystallization are also evident (Fig. 7C,D). Coarse mosaic calcite commonly fills pores, though microgranular calcite also occurs (Fig. 7C). Manganese dendrites (branched,

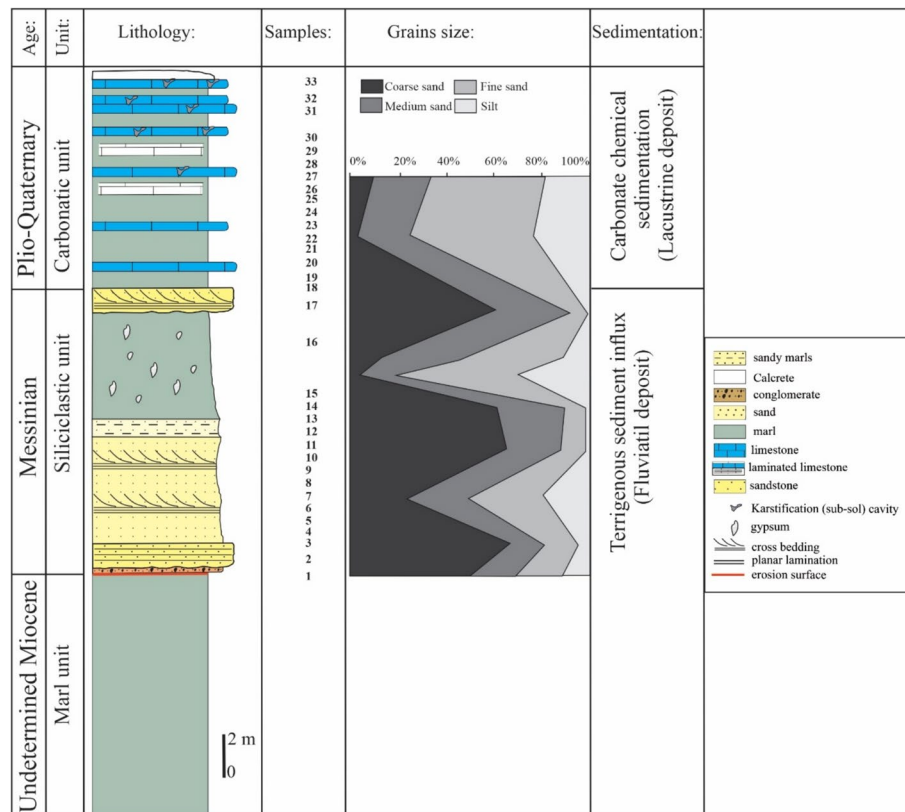


**Fig. 6** Stratigraphic log of Argoub Kemellal (Meguellati et al. 2025)

black structures formed during diagenesis) are widely distributed, particularly in pores and around grains (Fig. 7C). The presence of angular to sub-angular fine quartz grains and oxidized carbonate fragments (Fig. 7B) further confirms subaerial exposure and early diagenetic alteration. This microfacies is typical of fenestral carbonates, likely deposited in shallow lacustrine settings with periodic exposure.

The limestones exhibit evidence of early to moderate diagenetic alteration, including recrystallization to coarse mosaic calcite, infill of fenestrae by micrite and secondary calcite, and the development of manganese dendrites within pore spaces (Fig. 7C). While these features reflect post-depositional geochemical processes, they do not obscure primary sedimentary structures such as fenestrae, intraclasts, or desiccation cracks, which are key indicators of shallow lacustrine environments with periodic subaerial exposure.

### 3.2 Sedimentological analyses

The thin basal conglomeratic layer ( $\leq 10$  cm), composed of well-rounded clasts embedded in a sandy matrix, represents a localized high-energy lag deposit at the base of the succession. Its very limited thickness, combined with possible post-depositional reworking, explains the low gravel content (0.29%) recorded in the grain-size analyses. Above this basal level, the sediments are consistently dominated by sand, indicating a generally stable depositional energy regime throughout the section, with no pronounced fining-upward trend reflected in the granulometric data.

Grain-size analysis of the  $< 2$  mm fraction shows that sand is the major component (87.52%), subdivided into coarse (36.71%), medium (23.24%), and fine (24.51%) classes,

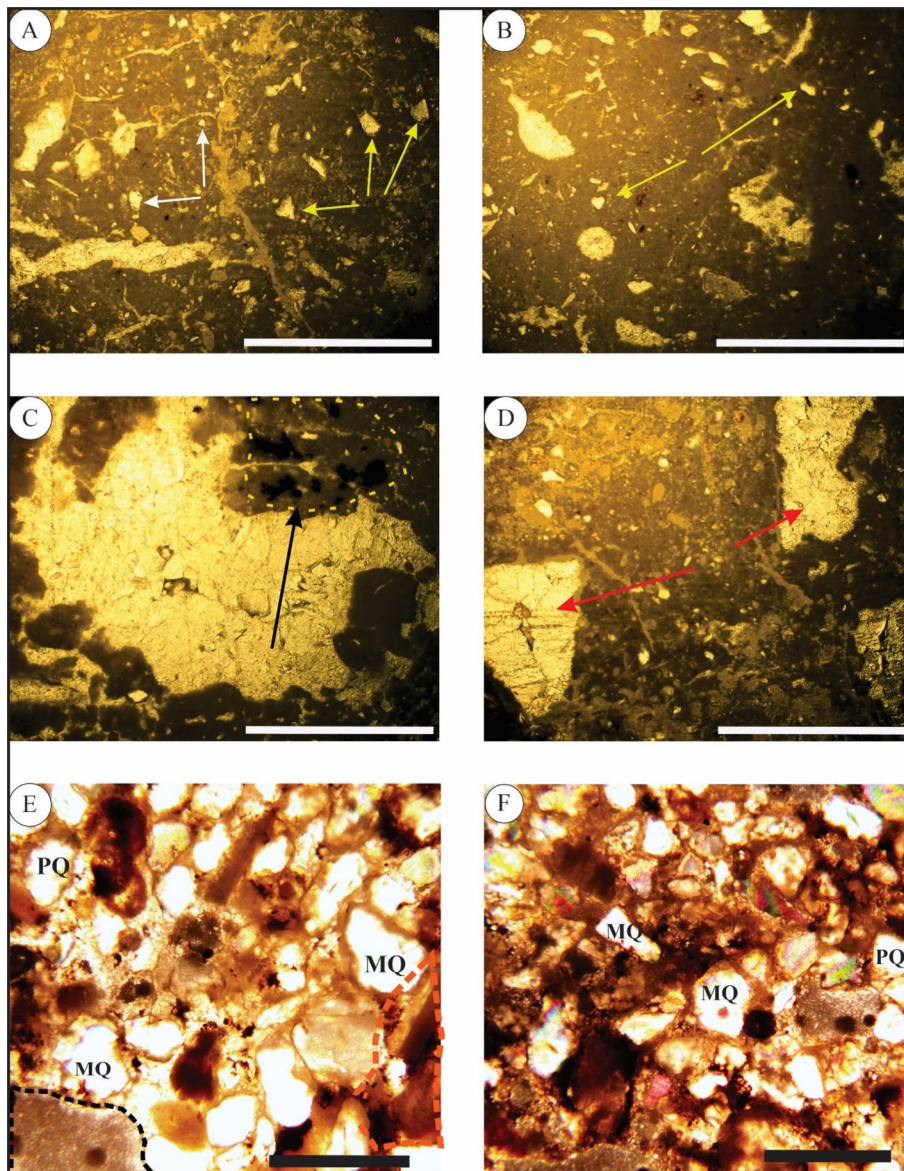


**Fig. 7** **A** and **B** Mudstone with angular grains of calcite (intraclasts, white arrows indicate quartz fine grains and calcite grains with yellow arrows). **A**: Fenestrae mudstone, intraclasts with yellow arrows, white arrows show fine grains of quartz, **B**: Intramicritic limestone, yellow arrows indicate intraclasts. Brownish-red oxidation in the center of microphotograph. **C**: Recrystallized Mudstone (black arrow indicate thin branching and concentrations of manganese dendrites, **C** and **D** coarse crystalline and mosaic calcite, red arrows show coarse crystalline, **C**: Coarse crystalline and mosaic calcite, the black arrow indicates manganese dendrites, **D**: Red arrows show a coarse crystalline and mosaic calcite. **E** and **F**: Photomicrographs of ferruginous sandstone, Quartz and interparticulate space; **PQ**: Polycrystalline quartz, **MQ**: monocrystalline quartz. Discontinuous red-line: ferruginous cement. Discontinuous black-line: argillitic cement. Note: Scale bar in all limestone photomicrographs is 3 mm

while silt accounts for 12.19%. (Fig. 6) Mean grain-size values range from 0.66 to 3.6  $\phi$ , corresponding to medium to fine sands. Sorting varies from 0.62 to 1.71  $\phi$  (moderately sorted), skewness ranges from  $-0.41$  to  $+0.43$   $\phi$  (predominantly symmetrical distributions), and kurtosis values (0.80 to 1.38  $\phi$ ) fall within mesokurtic ranges typical of natural sandy deposits.

Sand constitutes the dominant fraction throughout the stratigraphic column, showing small variation and indicating consistently high sand content in all samples. In contrast,

the silt fraction exhibits moderate variability, with noticeably lower proportions in samples 03, 09, 12 and 18. Grain-size parameters, including mean grain size, sorting, skewness, and kurtosis, display no significant systematic changes along the section.

### 3.3 Sedimentological parameters

Mean grain size ranges from 0.66 to 3.6  $\phi$ , indicating medium to fine sand. Sorting coefficients vary from 0.62 to 1.71  $\phi$ , suggesting moderate sorting. Skewness values ( $-0.41$  to  $+0.43$   $\phi$ ) indicate relatively symmetrical distributions. Kurtosis values (0.80 to 1.38  $\phi$ ) reflect mesokurtic distributions, typical of natural sands (Fig. 8). The ternary diagram (Fig. 9) confirms the sand-dominated nature of the sediments.

### 3.4 Calcimetric analysis

Calcium carbonate ( $\text{CaCO}_3$ ) content shows a clear stratigraphic trend. Values at the base of the section range from 13 to 32%, increasing toward the top where they reach 21% to 57%. Sample 30 records a progressive enrichment by the highest value of Calcium carbonates (Fig. 10).

### 3.5 Morphoscopy and exoscopy of Quartz grains

Morphoscopic analysis (Fig. 11) indicates a predominance of angular to sub-angular quartz grains ( $\sim 92\%$ ), with well-preserved edges. This suggests minimal transport and proximity to the sediment source. A smaller proportion of grains ( $\sim 7\%$ ) are sub-blunt to shiny, reflecting limited abrasion. Rounded and dull grains are rare ( $\sim 1\%$ ), further supporting a proximal origin with limited reworking.

Exoscopic examination reveals dissolution pits, surface desquamation, and siliceous coatings on grain surfaces. V-shaped percussion marks, characterized by concave impacts with sharp edges, are commonly observed. These features are homogeneously

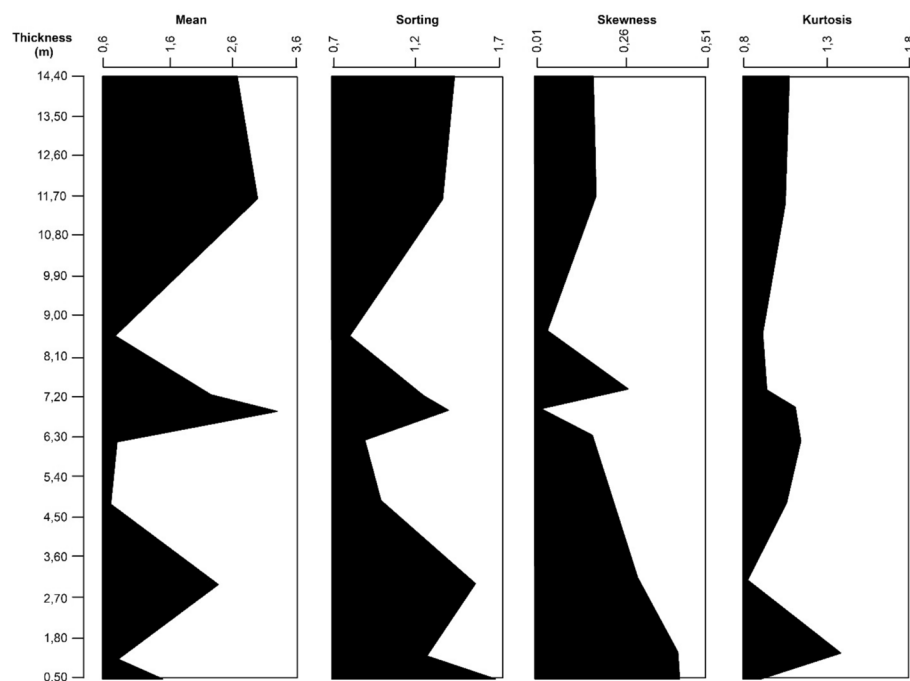


**Fig. 8** Variation of various sedimentological parameters according to the depth

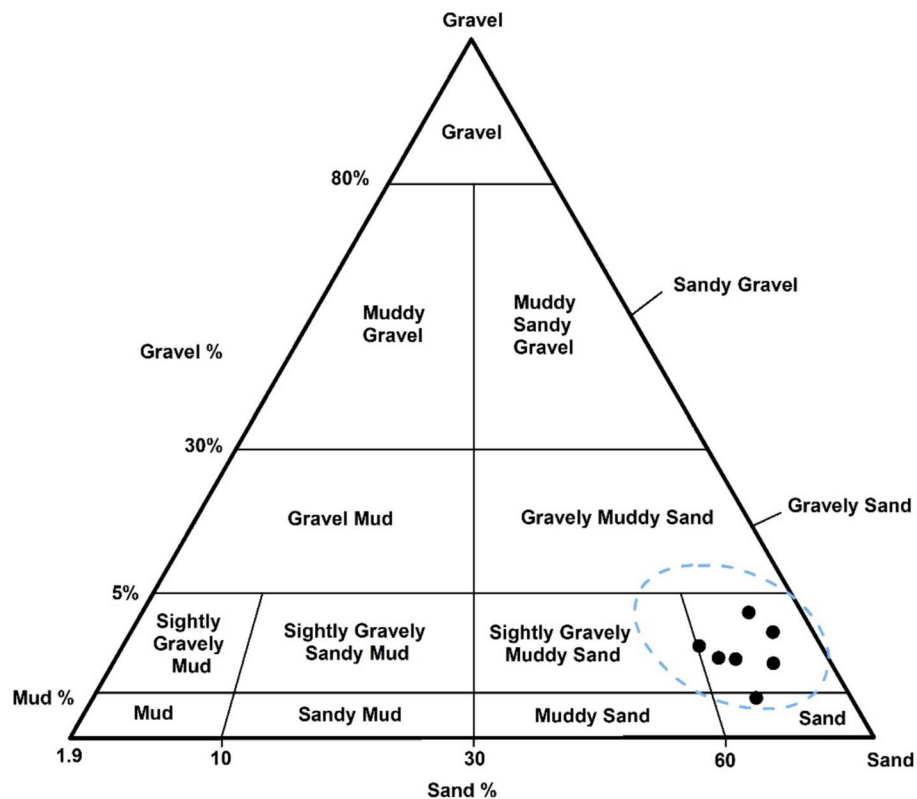


**Fig. 9** Ternary diagram of the grain size classification of the fine sediment (Argoub Kemellal section)

distributed across samples, suggesting uniform mechanical and chemical weathering processes (Fig. 12, 13).

Level 04: The presence of clear and blunted dissolution traces results from water circulation, indicating an undersaturated silica environment, thus a leached environment.

Level 06: Surface desquamation due to dissolution followed by the precipitation of silica in the form of films, indicating fluvial transport followed by stagnation or deposition of sediments.

V-shaped impact mark is visible, due to the collision of grains during transport (Fig. 14).

Level 08 (Marl): Surface desquamation due to dissolution, followed by the precipitation of silica in the form of thin films. These traces, being more pronounced, suggest fluvial transport followed by stagnation or sediment deposition.

Level 08 (Marly limestone): Multiple V-shaped impact marks are visible on this grain, indicating repeated grain collisions during transport. This suggests a fluvial environment, where the grains collide due to the water current.

#### 4 Discussion

The sedimentological analyses carried out on the Argoub Kemellal samples provide valuable insights into the origin and evolution of the studied sedimentary layers and their depositional settings.

Grain-size analysis reveals a broad spectrum of particle sizes across the stratigraphic layers, reflecting variable sediment sources and depositional energy levels. The presence of coarse sand grains suggests a short distance from the source area and deposition

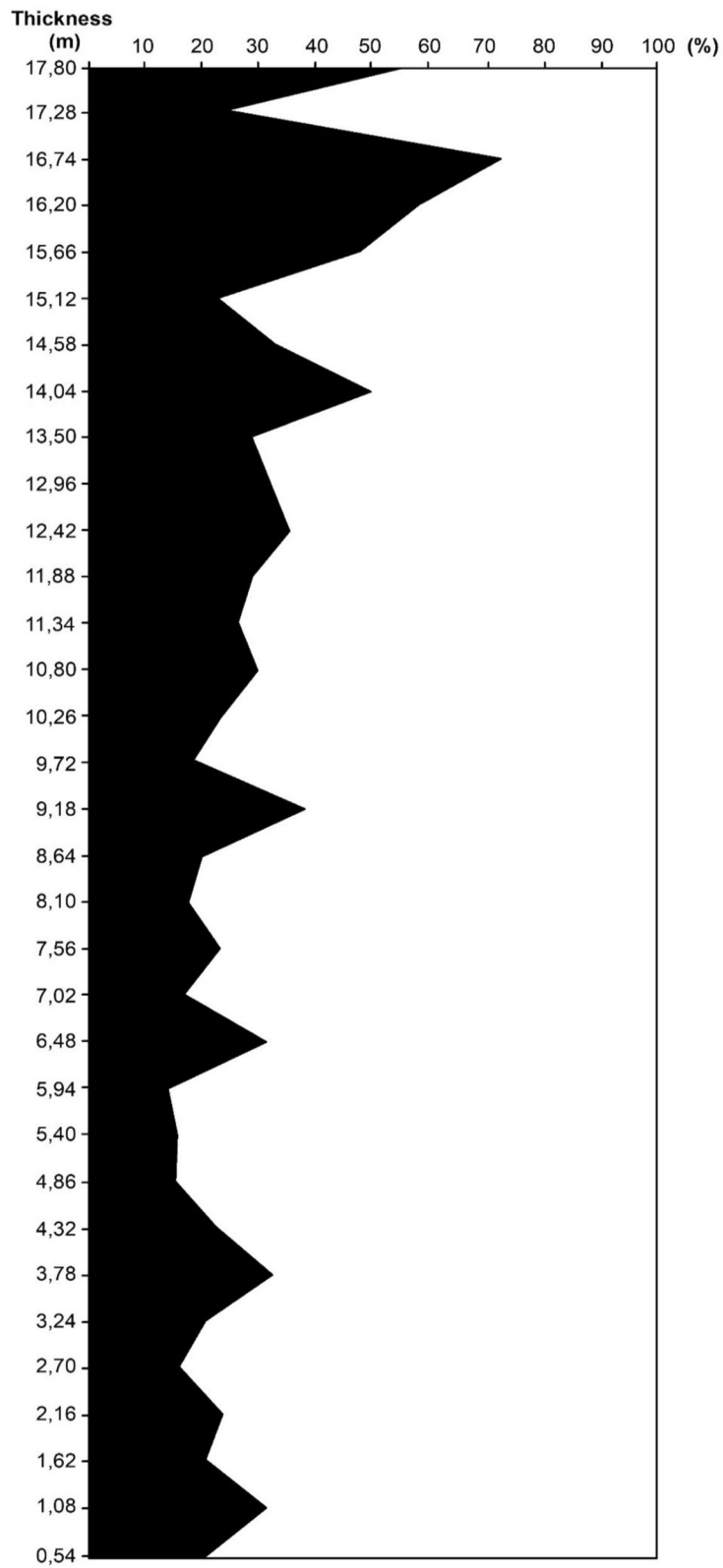


**Fig. 10** Variation of CaCO<sub>3</sub> content in the Argoub Kemellal section samples

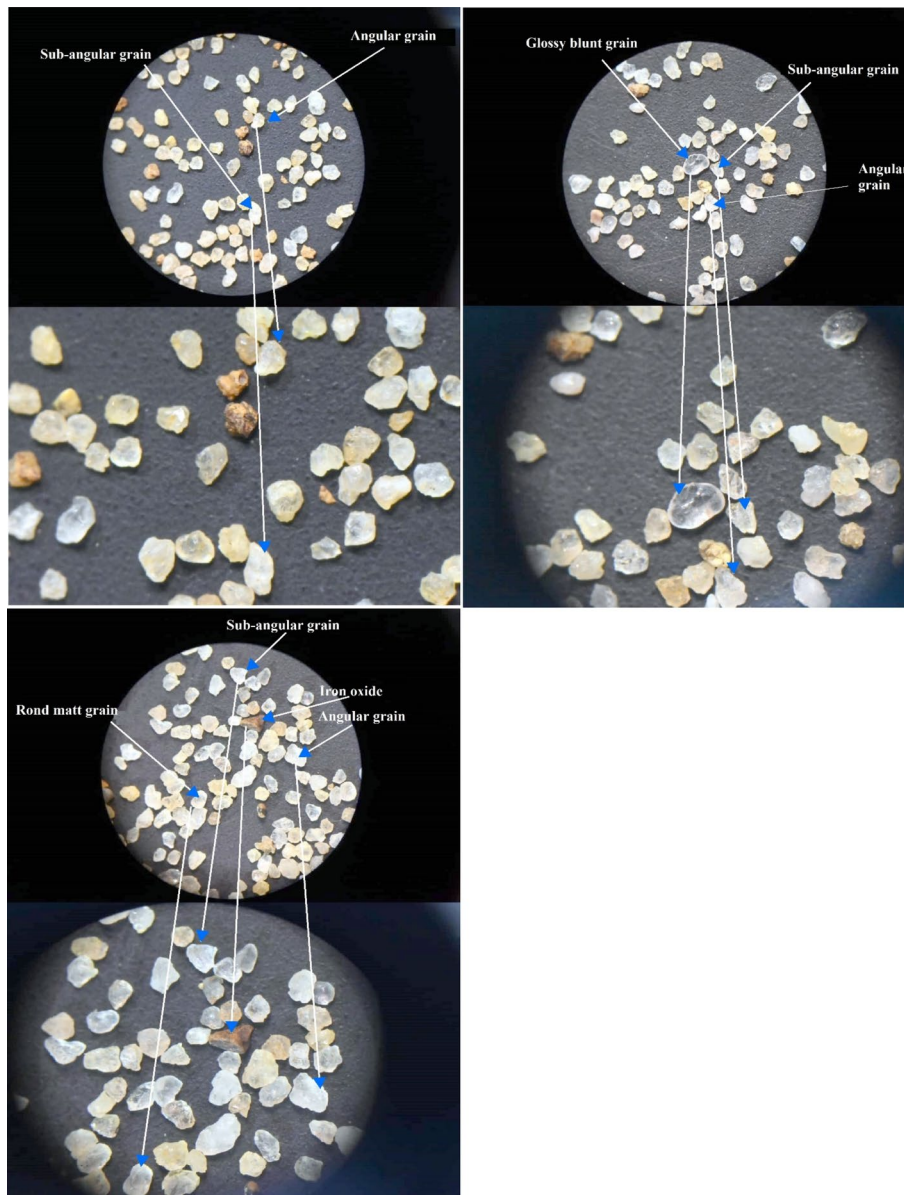


**Fig. 11** Morphoscopy of the sands from the Argoub Kemellal section (Magnification  $\times 50$ ). (Sample 05, 10, 20)

was under high-energy conditions, likely within a fluvial context. In contrast, finer sand grains may have undergone longer transport and weathering, originating from more distal sources and deposited under lower-energy conditions.

#### 4.1 Grain size distribution and sedimentary dynamics

The progression from coarse to fine grain sizes in the sandstone units (from coarse quartz in Level 03 to finer textures in Level 07) indicates a gradual shift from a high-energy fluvial regime to a quieter depositional environment, potentially associated with increased accommodation space within the basal siliciclastic system. This transition is followed by the establishment of carbonate sedimentation, marking a reduction in detrital input and the onset of a chemically dominated depositional regime indicative of lacustrine influence.

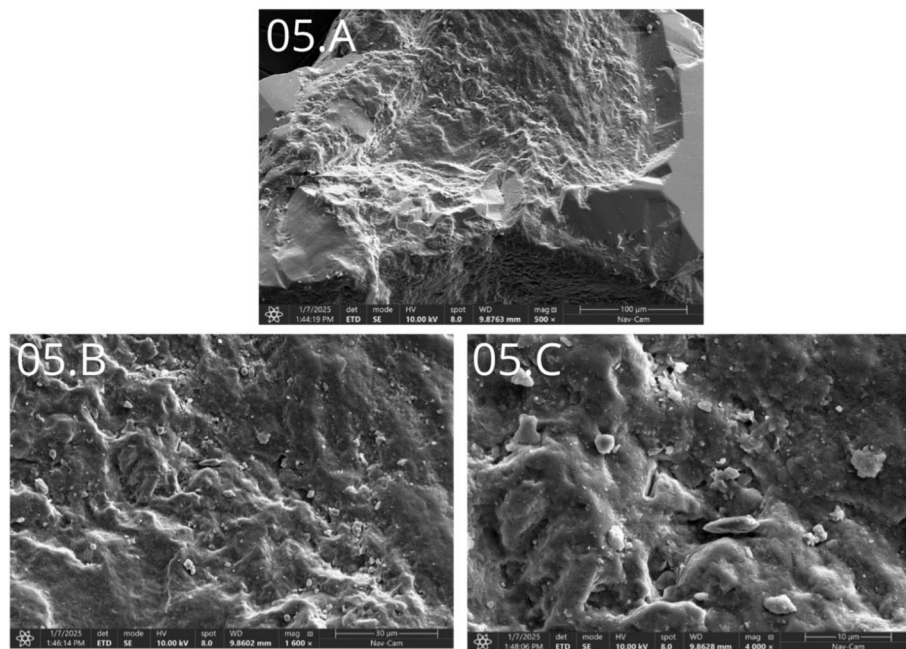


**Fig. 12** SEM Observations of Level 04 (Sample 05) Surface at Different Magnifications

#### 4.2 Carbonate content and depositional evolution

The predominance of coarse grains, coupled with moderate sorting, indicates deposition in a setting subject to fluctuating transport energy, likely linked to seasonal variations in fluvial discharge. Although the sorting values are moderate, they indicate partial hydraulic sorting. This intermediate sorting pattern is consistent with deposition under periodic changes in flow conditions, such as episodic flooding.

Skewness values near (zero) indicate symmetrical grain-size distributions, supporting the interpretation of a generally stable depositional regime with limited fluctuations in sediment supply. Kurtosis values close to (one) (mesokurtic) reflect grain-size distributions comparable to natural sands with slightly peaked tendencies. Collectively, the grain-size data indicate a sedimentary system progressively evolving from a proximal, high-energy fluvial environment toward a more distal, lower-energy setting increasingly influenced by lacustrine conditions.

Calcimetric analysis reveals a progressive increase in calcium carbonate ( $\text{CaCO}_3$ ) content from the base to the top of the section. This upward trend reflects a shift toward depositional conditions favoring chemical precipitation of carbonates. The decrease in detrital input and the rise in carbonate content indicate a transition from a siliciclastic-dominated system to one in which chemical processes become increasingly important.

This enrichment in  $\text{CaCO}_3$  suggests a gradual evolution from fluvial deposition toward more stable standing-water environments where carbonate precipitation dominates. The formation of calcareous crusts in the upper part of the sequence is consistent with prolonged episodes of reduced clastic influx and enhanced carbonate accumulation in a relatively calm lacustrine setting.

#### 4.3 Paleoenvironmental conditions

Morphoscopic analysis highlights the dominance of angular to sub-angular quartz grains (approximately 92%), indicating limited transport distance and minimal abrasion. This

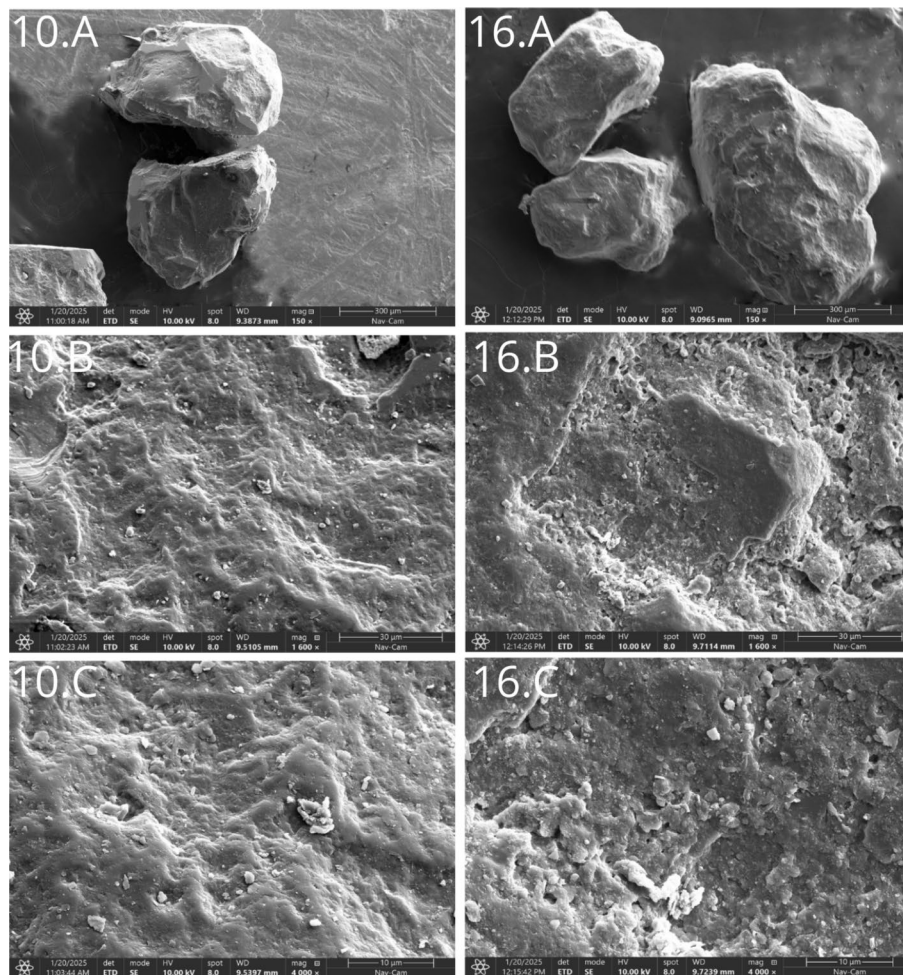


**Fig. 13** SEM Observations of the Surfaces of level 04 (Sample 10), and level 06 (sample 16) at Different Magnifications

morphology suggests a proximal source and rapid deposition consistent with a fluvial system operating near its sediment supply area. The presence of a small proportion of shiny, blunt, and sub-blunt grains (about 07%) indicates limited reworking under moderate energy conditions, likely related to episodic fluvial transport. Rounded and dull grains are rare (01%), further supporting short transport paths and minimal sediment recycling.

Exoscopic analysis reinforces these observations. Sand grains exhibit clear but blunt dissolution traces with desquamation in sheltered areas, indicating fluvial transport followed by sediment stagnation or deposition, as evidenced by the presence of silica films in a leached environment. V-shaped percussion marks reflect mechanical impacts typical of high-energy fluvial conditions, while dissolution features, desquamation, and siliceous coatings on quartz grains indicate post-depositional chemical alteration. The coexistence of mechanical and chemical surface features suggests alternating phases of energetic transport and subsequent chemical modification, implying the combined influence of fluvial processes and later interaction with standing water or groundwater.

Collectively, the sedimentological, morphoscopic, and exoscopic data support a depositional evolution from a fluvial siliciclastic system toward a lacustrine-influenced

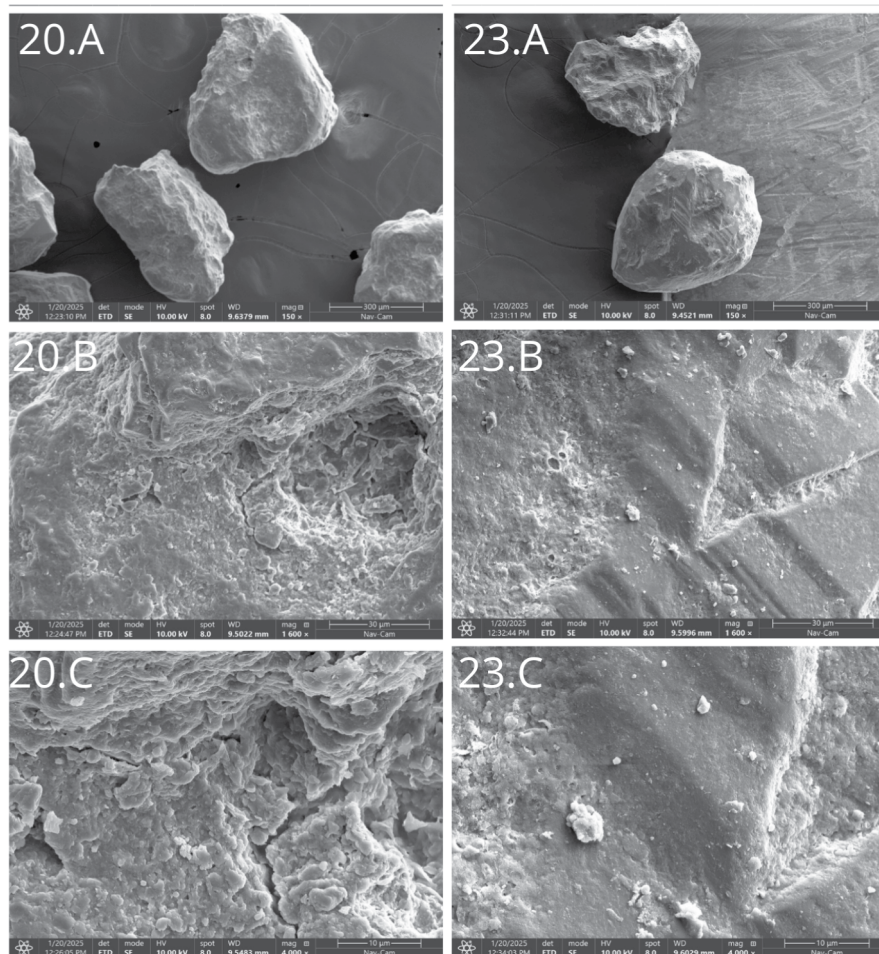


**Fig. 14** SEM Observations of the Surfaces of Level 08 (Samples 20 and 23) at Different Magnifications

environment, characterized by reduced detrital supply and enhanced carbonate precipitation. While local neotectonic activity may have contributed to variations in sediment influx and accommodation space, the observed sedimentary patterns suggest that environmental change was the primary driver. Periods enriched in coarse siliciclastics may reflect short-term tectonic pulses, whereas intervals dominated by finer sediments or carbonates indicate reduced tectonic influence and relative basin deepening. This distinction allows us to separate tectonic signals from climatic forcing, attributing facies continuity, grain-size distributions, and carbonate accumulation primarily to climate-driven processes.

The findings are consistent with previous regional studies [18–20], highlighting environmental changes that prompted the Neogene-Quaternary fluvio-lacustrine transition. Notably, the age of the Argoub Kemellal transition appears slightly younger than in neighboring regions of Tunisia [25, 26] and Morocco [27]. This diachronous pattern may reflect differences in local basin response times to regional climate forcing or subtle topographic or structural controls that modulated sedimentation rates. Such a rationale clarifies why local variations exist and frames potential directions for future research.

Similar Neogene-Quaternary environmental transitions have been documented elsewhere, including in Pakistan, supporting the broader significance of these depositional patterns [1–16, 44, 50, 51]. Regionally correlatable deposits in Tunisia, Algeria, and Morocco, such as Late Miocene marls and evaporites from continuous foredeep settings across the Rif–Tell–Cap Bon domains (e.g., Guercif Basin in Morocco, Gulf of Hammamet in Tunisia, and Bas Chelif in Algeria) [52, 53], correspond to a marly-limestone unit in Argoub Kemellal, where the Messinian crisis is not recorded. Overlying Plio-Quaternary coastal to shallow marine sands, including raised marine sediments and coquina levels, are also regionally correlatable [54], whereas in Oum El Bouaghi, lacustrine deposits are preserved [55].

The Neogene-Quaternary deposits in the studied section differ from the regional successions, reflecting local variations in depositional environments likely controlled by a combination of climate-driven processes and localized tectonic adjustments. This distinction strengthens the interpretation of sedimentological records as primarily climatically modulated while acknowledging the influence of tectonic factors.

## 5 Conclusion

The integrated sedimentological and petrographic analysis of the Argoub Kemellal section provides a detailed reconstruction of the environmental evolution of the Oum El Bouaghi region throughout the Neogene–Quaternary period. The stratigraphic succession documents a dynamic history shaped by the interplay of fluvial, lacustrine, and palustrine systems.

The lower part of the section, dominated by marls, conglomerates, and coarse sandstones, reflects the onset of a high-energy fluvial phase. The abundance of angular and sub-angular quartz grains, together with cross-bedded sandstone layers, indicates rapid deposition from nearby sources with minimal transport or reworking. These features point to episodic, high-intensity flood events typical of alluvial environments close to active sediment supply zones. Upward in the sequence, the gradual transition toward finer-grained deposits such as sandy marls and compacted sands marks a reduction in hydrodynamic energy. This evolution suggests the progressive decline of fluvial influence and the establishment of more stable settings, including floodplains or shallow water bodies. The fining-upward pattern captures a shift toward lower-energy depositional conditions.

The upper portion of the profile, consisting of alternating marl and limestone layers along with well-developed carbonate horizons, reveals a transition toward shallow lacustrine to palustrine environments. Petrographic evidence fenestral textures, intraclasts, desiccation features, and traces of subaerial exposure indicates deposition in intermittently emergent settings affected by fluctuating water levels. Manganese dendrites and oxidation structures further reflect local weathering processes. The significant increase in carbonate content, confirmed by calcimetric data, supports enhanced precipitation in shallow basins. Morphoscopic and exoscopic characteristics of quartz grains, including angular forms, reinforce the interpretation of limited transport and localized depositional processes.

Overall, the Argoub Kemellal section provides a valuable record of the interactions between tectonics and sedimentary processes. It offers important insights into the

## Neogene–Quaternary paleoenvironmental evolution of northeastern Algeria and serves as a solid reference for regional paleogeographic reconstructions.

### Author contributions

Meguellati Asma Djerrab Abderrezak Khiari Abdelkader Gallet Xavier Dinar Haythem Garah Abdelmomen Riheb Hadji : Conceptualisation, Methodology, Investigation, Formal analysis, Visualisation – original draft., Imtiyaz Akbar Najar, Raudhah Ahmadi, Nadeem A Khan: Writing – review & editing, Methodology, Supervision, Software, Supervision, Data curation, Validation, Supervision, Project administration.

### Funding

Open Access funding provided by Universiti Malaysia Sarawak. This research did not receive any funding.

### Data availability

The data supporting the findings of this study are available from [Meguellati Asma]. While some data are under license and cannot be made fully public, all data necessary to reproduce the results can be obtained from the authors upon reasonable request. Additional supporting information is provided in the Supplementary Index accompanying this manuscript.

### Declarations

#### Ethical approval and consent to participate

Not applicable.

#### Consent for publication

Not applicable.

#### Competing interests

The authors declare no competing interests.

### Author details

<sup>1</sup>Laboratory of Natural Resources and Management of Sensitive Environments (LRNAMS), Department of Geology, Faculty of Earth Sciences and Architecture, Larbi Ben M'hidi University, Oum El Bouaghi, Algeria

<sup>2</sup>Faculty of Humanities and Social Sciences, Department of Archaeology, University of Guelma 8 May 1945, BP 401, 24000 Guelma, Algeria

<sup>3</sup>Department of Prehistory, National Museum of Natural History, 1 Rue René Panhard, 75013 Paris, France

<sup>4</sup>Centre de Recherche en Aménagement de Territoire (CRAT), Campus Zouaghi Slimane, Constantine, Algérie

<sup>5</sup>Department of Geology, Institute of Earth and Universe Sciences, University of Batna 2, 53, Constantine Road, 05078 Fesdis, Batna, Algeria

<sup>6</sup>Laboratory of Applied Research in Engineering Geology, Geotechnics, Water Sciences, and Environment, Department of Earth Sciences, Institute of Architecture and Earth Sciences, University of Farhat Abbas, Setif, Algeria

<sup>7</sup>Faculty of Engineering, Universiti Malaysia Sarawak, 94300 Kota Samarahan, Sarawak, Malaysia

<sup>8</sup>Civil Engineering Department, College of Engineering, King Khalid University, 61421 Abha, Saudi Arabia

Received: 5 September 2025 / Accepted: 27 January 2026

Published online: 07 February 2026

### References

1. Bendaoud A, et al. The geology of North Africa. Springer; 2024.
2. Chalouan A, Michard A, El Kadiri K. Punctuated Neogene tectonics and stratigraphy of the African-Iberian plate boundary zone: concurrent development of Betic-Rif basins. *Netherlands J Geosci*. 2019;98:1–15.
3. Mehmood M, Naseem AA, Saleem M, Rehman Ju, Kontakiotis G, Janjuhah HT, et al. Sedimentary facies, architectural elements, and depositional environments of the Maastrichtian Pab Formation in the Rakhi Gorge, Eastern Sulaiman Ranges, Pakistan. *J Mar Sci Eng*. 2023;11:726. <https://doi.org/10.3390/jmse11040726>.
4. Zaheer M, Khan MR, Mughal MS, Janjuhah HT, Makri P, Kontakiotis G. Petrography and lithofacies of the Siwalik Group in the core of Hazara-Kashmir Syntaxis: implications for middle stage Himalayan orogeny and paleoclimatic conditions. *Minerals*. 2022;12:1055. <https://doi.org/10.3390/min12081055>.
5. Bilal A, Mughal MS, Janjuhah HT, Ali J, Niaz A, Kontakiotis G, et al. Pétrographie et provenance de la formation sub-himalayenne de Kuldana : implications pour le contexte tectonique et les conditions paléoclimatiques. *Minerals*. 2022;12:794. <https://doi.org/10.3390/min12070794>.
6. Qamar S, Shah MM, Janjuhah HT, Kontakiotis G, Shahzad A, Besiou E. Sedimentological, diagenetic, and sequence stratigraphic controls on the shallow to marginal marine carbonates of the middle Jurassic Samana Suk Formation, North Pakistan. *J Mar Sci Eng*. 2023;11:1230. <https://doi.org/10.3390/jmse11061230>.
7. Agiadi K, Antonarakou A, Kontakiotis G, et al. Connectivity controls on the late Miocene eastern Mediterranean fish fauna. *Int J Earth Sci (Geol Rundsch)*. 2017;106:1147–59. <https://doi.org/10.1007/s00531-016-1355-7>.
8. Karakitsios V, Roveri M, Lugli S, Manzi V, Gennari R, Antonarakou A, et al. A record of the messinian salinity crisis in the eastern Ionian tectonically active domain (Greece, eastern Mediterranean). *Basin Res*. 2017;29(2):203–33. <https://doi.org/10.1111/bre.12173>.
9. Karakitsios V, Cornée J-J, Tsourou T, Moissette P, Kontakiotis G, Agiadi K, et al. Messinian salinity crisis record under strong freshwater input in marginal, intermediate, and deep environments: the case of the North Aegean. *Palaeogeogr Palaeoclimatol Palaeoecol*. 2017;485:316–35. <https://doi.org/10.1016/j.palaeo.2017.06.023>.

10. Kontakiotis G, Butiseacă G-A, Karakitsios V, Antonarakou A, Zarkogiannis S, Agiadi K, et al. Hypersalinity accompanies tectonic restriction in the eastern Mediterranean prior to the Messinian Salinity Crisis. *Palaeogeogr Palaeoclimatol Palaeoecol*. 2022;592(2):110903. <https://doi.org/10.1016/j.palaeo.2022.110903>.
11. Zachariasse WJ, Kontakiotis G, Lourens LJ, Antonarakou A. The messinian of Agios Myron (Crete, Greece): a key to better understanding diatomite formation south of Crete, on Gavdos Island. *Palaeogeogr Palaeoclimatol Palaeoecol*. 2021;581:110633. <https://doi.org/10.1016/j.palaeo.2021.110633>.
12. Butiseacă GA, van der Meer MTJ, Kontakiotis G, Agiadi K, Thivaoui D, Besiou E, et al. Multiple crises preceded the Mediterranean Salinity Crisis: aridification and vegetation changes revealed by biomarkers and stable isotopes. *Glob Planet Change*. 2022;217:103951. <https://doi.org/10.1016/j.gloplacha.2022.103951>.
13. Drinia H, Antonarakou A, Kontakiotis G. On the occurrence of early Pliocene marine deposits in the Ierapetra Basin, eastern Crete, Greece. *Bull Geosci*. 2008;83(1):63–78.
14. Kontakiotis G, Karakitsios V, Mortyn PG, Antonarakou A, Drinia H, Anastasakis G, et al. New insights into the early Pliocene hydrographic dynamics and their relationship to the climatic evolution of the Mediterranean Sea. *Palaeogeogr Palaeoclimatol Palaeoecol*. 2016;459:348–64.
15. Agiadi K, et al. The marine biodiversity impact of the Late Miocene Mediterranean salinity crisis. *Science*. 2024;385:986–91. <https://doi.org/10.1126/science.adp3703>.
16. Agiadi K, et al. Late Miocene transformation of Mediterranean Sea biodiversity. *Sci Adv*. 2024;10:eadp1134. <https://doi.org/10.1126/sciadv.adp1134>.
17. Voute C. Geological synthesis of the areas surrounding Ain Fakroun, Ain Barouche, and neighboring regions: Detailed description of the Ain Fakroun and Ain Babouche map sheets (1:50,000). *Serv Géol Algérie*, 1967.
18. Rebouh N, Belkendil A, Tout F, Dinar H, Benzid Y, Zeghmar A, et al. Landslide susceptibility assessment using hybrid geo-spatial, frequency ratio, and AHP models in Souk Ahras province, Northeastern of Algeria. *Sci Rep*. 2026;16:2288. <https://doi.org/10.1038/s41598-025-32062-2>.
19. Coiffait PE. Un bassin post-nappe dans son cadre structural : l'exemple du bassin de Constantine (Algérie nord-orientale). Doctoral dissertation, Université Nancy 1, 1992.
20. Marmi R. Les bassins continentaux de l'avant-pays de la chaîne alpine de l'Algérie nord-orientale : étude stratigraphique, sédimentaire, structurale et géochimique. Doctoral dissertation, Université Nancy 1, 1996.
21. Tout F, Rebouh N, Dinar H, Zouak Z, Benzid Y. The issue of using annual rainfall maps in multi-criteria analysis to identify flood-prone areas. *Geomat Landman landsc*. 2024;4:267–78. <https://doi.org/10.15576/GLL/195555>.
22. Oudni A, Dinar H, Zedam R. Caractérisation géologique et géotechnique de la cuvette du barrage Tagharist, 2016.
23. Mansouri Z, Dinar H, Belkendil A, Bakelli O, Drias T, Assadi AA, et al. Integrated groundwater quality assessment for irrigation in the Ras El-Aioun District: combining IWQI, GIS, and machine learning approaches. *Water*. 2025;17(11):1698. <https://doi.org/10.3390/w17111698>.
24. Nouali H, Bouroubi-Ouadfel Y, Moulla AS, Mutlu H, Vaselli O, Dinar H, et al. Hydrogeochemical and isotopic characterization of the El-Tarf geothermal aquifer (Algerian–Tunisian border): implications of the regional geodynamic structure and the water–rock interactions. *J Afr Earth Sci*. 2025;223:105523. <https://doi.org/10.1016/j.jafrearsci.2024.105523>.
25. Ghannem N, Tlili F, Riahi C, Regaya K. Étude sédimentologique des dépôts carbonatés continentaux de type palustre de la région de Tazerouine, Nord-Ouest de la Tunisie. *Carnets Geol*. 2016;16:43.
26. Tlili F, Regaya K. Les dépôts carbonatés continentaux de la région de Hajeb El Ayoun (Tunisie centrale): implications paléoenvironnementales et morphologiques. *Physio-Géo*. 2019;13:133–53. <https://doi.org/10.4000/physio-geo.8316>.
27. El Harfi A, Lang J, Verrecchia E, Durllet C, Landreine P, Chellai EH, et al. Origine pédo-diagénétique de la calcite fibreuse pseudosphérolitique (pseudo-Microcodium) du Paléogène continental palustre dans le bassin d'Anzal (Anti Atlas, Maroc). *Afr Geosci Rev*. 2006;13:447–69.
28. Najjar IA, Ahmadi RB, Jamian MAH, Hamza HB, Ahmad A, Sin CH. Site-specific ground response analysis using the geotechnical dataset in moderate seismicity region. *Int J Mech*. 2022;16(1):37–45.
29. Foresi LM, Baldassini N, Sagnotti L, Lirer F, Di Stefano A, Caricchi C, et al. Integrated stratigraphy of the St. Thomas section (Malta Island): a reference section for the lower Burdigalian of the Mediterranean Region. *Mar Micropaleontol*. 2014;111:66–89. <https://doi.org/10.1016/j.marmicro.2014.06.004>.
30. Laouini H, Hacini M, Cherif A, Remita A. Sedimentological and paleoenvironmental analysis of Chott Baghdad deposit (Northern Algerian Sahara). *Energy Procedia*. 2019;157:59–67.
31. Chellat S, Toubal L, Djerrab A, Bourefis A, Hamdi-Aïssa B, Salmi-Laouar S. Molluscan and sedimentological sequences of the late Quaternary deposits of Morsott region (NE Algeria) and their paleoenvironmental implication. *BSGF-Earth Sci Bull*. 2018;189:17. <https://doi.org/10.1051/bsgf/2018016>.
32. Chellat S. Some problems of the application of the U–Th series and radiocarbon absolute dating techniques to Quaternary fluviolacustrine deposits in the Morsott commune of Algeria. *Archaeol Anthropol Sci*. 2021;13:76. <https://doi.org/10.1007/s12520-021-01319-y>.
33. Najjar IA, Ahmadi R, Amuda AG, Mourad R, Bendary NE, Ismail I, et al. Advancing soil-structure interaction (SSI): a comprehensive review of current practices, challenges, and future directions. *J Infrastruct Preserv Resil*. 2025;6(1):5.
34. Djaiz F, Defaflija N, Lamouri B, Boushaba A, Chairat I. Quaternary fluvial terrace of the Oued El Gourzi (Batna, NE Algeria): sedimentology and characteristics of the depositional environment. In: *Paleobiodiversity and tectono-sedimentary records in the mediterranean tethys and related eastern areas*. Springer; 2019. p. 331–4.
35. Defaflija N, Djaiz F, Fehdi C. Paleoenvironmental study of Oum Ali region (Tébessa, Algeria) during Quaternary, through the study of fluvial terrace of Khenigue Wadi. *Acta Geobalkanica*. 2021. <https://doi.org/10.18509/AGB217-40153n>.
36. Rabahi N, et al. The vertical distribution of the alluvial chemo-facies of Boumerzoug Wadi, Constantine, Northeastern Algeria: paleoenvironmental significance and climate evolution. *An Univ Oradea Ser Geogr*. 2021;31:68–79. <https://doi.org/10.30892/auog.311108-865>.
37. Dinar H, Khiari A, Mansouri Z, Taib H, Nouali H, Boumaza B. Uplifted marine terraces by active coastal tectonic deformation along the east of Algiers: implications for African and European plate convergence and sea-level curves. *Bol Geol Min*. 2023;134:57–67. <https://doi.org/10.21701/bolgeomin/134.2/004>.
38. Haythem DINAR. Characterization of Quaternary Deposits and Deformations in Eastern Algeria. Case of the Coastal Formations (Doctoral dissertation, University of Batna), 2023.

39. Bekhouch G, Puckett TM, Khiari A, Djerrab MR, Meguellati A, Dinar H. Optimized event stratigraphy of Cenomanian-Turonian ostracods of North Africa and the Middle East. *J Afr Earth Sci.* 2023;208:105061. <https://doi.org/10.1016/j.jafrearsci.2023.105061>.
40. Courty MA, Fedoroff N, Guilloiré P. Micromorphologie des sédiments archéologiques. In *Géologie de la préhistoire: méthodes, techniques, applications*, p. 439–477 (Association pour l'Étude de l'Environnement, Paris, 1987).
41. Guilloiré P. *Méthode de fabrication mécanique et en série de lames minces*. Département Sols, Institut National Agronomique, 1983.
42. Folk RL, Ward WC. Brazos River bar (Texas): a study in the significance of grain size parameters. *J Sediment Res.* 1957;27:3–26.
43. Rivière A. *Méthodes granulométriques: techniques et interprétations*. Paris: Masson; 1977.
44. Najari IA, Ahmadi R, Mourad R, Bendary NE, Tang S, Ahmad A, et al. Laboratory investigation of soil suffusion through particle size distribution and hydraulic conductivity analysis. *Iran J Sci Technol Trans Civ Eng.* 2025. <https://doi.org/10.1007/s40996-025-01780-y>.
45. Anderson JR. Sand sieve analysis. In: Gore PJW (editors) *Historical Geology Online Laboratory Manual*, 278 (Department of Geology, Georgia Perimeter College, 2007).
46. Miskovsky JC, Debarb E. Granulométrie des sédiments et étude de leur fraction grossière. In *Géologie de la Préhistoire : méthodes, techniques, applications*, p. 479–500 (Géopré, Perpignan, 2002).
47. Cailleux A, Tricart J. *Initiation à l'étude des sables et des galets*, vol. 5. Paris: CDU; 1959.
48. Le Ribault L. *L'exoscopie du quartz*. Paris: Masson; 1977.
49. Le Ribault L, Giresse P. Contribution de l'étude exoscopique des quartz à la reconstitution paléogéographique des derniers épisodes du Quaternaire littoral du Congo. *Quat Res.* 1981;15:86–100.
50. Mahran T, Hassan AM. Controls on Late Miocene to Early Quaternary continental sedimentation during the development of the Sohag basin, Nile Valley. *Egypt J Afr Earth Sci.* 2023;199:104829.
51. Mahran T. The Late Oligocene–Early Pleistocene paleoclimatic pattern in the northeastern Sahara, Sohag Basin, Egypt: evidence from lithofacies and pedogenic features. *Arab J Geosci.* 2024;17:250.
52. Sani F. *Neogene–Quaternary evolution of the Guercif Basin (NE Morocco)*, 2000.
53. Brahim GB. *Neogene tectono-stratigraphic evolution of the Gulf of Hammamet (Tunisia)*, 2013.
54. Schwarzans W. *Stratigraphy of Neogene–quaternary shallow-marine units in NW Africa*, 2023.
55. Tucker ME. *Sedimentary rocks in the field: a practical guide*. 3rd ed. Chichester: Wiley; 2001. p. 234.

### Publisher's Note

Springer Nature remains neutral with regard to jurisdictional claims in published maps and institutional affiliations.